Effect of strain, magnetic field and field angle on the critical current density of Y $Ba_2Cu_3O_{7-\delta}$ coated conductors

2010 Supercond. Sci. Technol. 23 072001

(http://iopscience.iop.org/0953-2048/23/7/072001)

Supercond. Sci. Technol. **23** (2010) 072001 (7pp) doi:10.1088/0953-2048/23/7/072001

RAPID COMMUNICATION

Effect of strain, magnetic field and field angle on the critical current density of $YBa_2Cu_3O_{7-\delta}$ coated conductors*

D C van der Laan[1,2], J W Ekin[1,2], J F Douglas[2], C C Clickner[2], T C Stauffer[2] and L F Goodrich[2]

[1] Department of Physics, University of Colorado, Boulder, CO 80309, USA
[2] National Institute of Standards and Technology, Boulder, CO 80305, USA

E-mail: danko@boulder.nist.gov

Received 25 March 2010, in final form 30 April 2010
Published 18 May 2010
Online at stacks.iop.org/SUST/23/072001

Abstract
A large, magnetic-field-dependent, reversible reduction in critical current density with axial strain in $YBa_2Cu_3O_{7-\delta}$ coated conductors at 75.9 K has been measured. This effect may have important implications for the performance of $YBa_2Cu_3O_{7-\delta}$ coated conductors in applications where the conductor experiences large stresses in the presence of a magnetic field. Previous studies have been performed only under tensile strain and could provide only a limited understanding of the in-field strain effect. We now have constructed a device for measuring the critical current density as a function of axial compressive and tensile strain and applied magnetic field as well as magnetic field angle, in order to determine the magnitude of this effect and to create a better understanding of its origin. The reversible reduction in critical current density with strain becomes larger with increasing magnetic field at all field angles. At 76 K the critical current density is reduced by about 30% at −0.5% strain when a magnetic field of 5 T is applied parallel to the *c*-axis of the conductor or 8 T is applied in the *ab*-plane, compared to a reduction of only 13% in self-field. Differences in the strain response of the critical current density at various magnetic field angles indicate that the pinning mechanisms in $YBa_2Cu_3O_{7-\delta}$ coated conductors are uniquely affected by strain.

1. Introduction

Progress in $YBa_2Cu_3O_{7-\delta}$ (YBCO) coated conductor development [1, 2] has made large-scale electric power grid applications possible. To guarantee the success of these and other applications, we must determine the limits of the conductors under their operating conditions. For instance, YBCO coated conductors experience large axial stresses in high-field magnets, motors and generators. The YBCO layer breaks at a tensile strain defined by the irreversible strain limit (ε_{irr}), which should not be exceeded in applications [3–6]. The irreversible strain limit in YBCO coated conductors under axial compression remains unknown, but most likely exceeds the level of axial compressive strain that a conductor would experience in typical applications [7]. Other conductor failure modes that may occur in applications include delamination of the YBCO layer under transverse tensile stress [8], and in-plane bending [9], which occurs in certain cable configurations.

Strain affects the performance of the YBCO coated conductor even before the ceramic superconducting layer breaks. A reversible degradation of the critical current density (J_c) with axial strain has been measured in self-field [4, 10, 11] and exceeds 40% under −1% axial compression [12]. Recent studies have shown that strain also affects the in-field performance of YBCO coated conductors [13–16], but a limited understanding of this effect has been obtained, because measurements were performed under tensile strain only. A

* Contribution of NIST, not subject to US copyright.

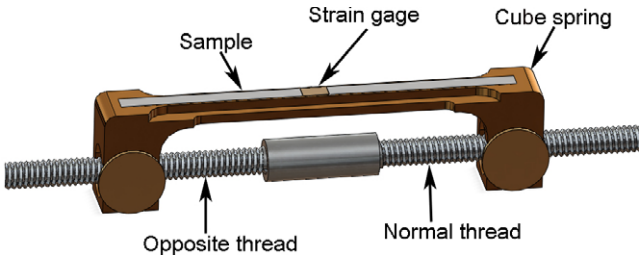

Figure 1. Compact bending spring with a sample mounted on top of the patterned bridge. A double-threaded rod passes through threaded bushings, which strains the spring. A strain gauge is mounted on top of the sample (shown), and a second on the bottom of the spring (not shown) to measure the strain in the sample.

more detailed understanding of the effect of strain on the in-field performance can be obtained only when the effect of axial compressive strain is also taken into account, as we shall demonstrate here.

YBCO coated conductors contain a complex pinning landscape in which the pinning strength depends on the orientation of the magnetic field [17–24]. It is important to measure the intrinsic strain effect in different magnetic field angles to allow us to understand how strain affects the various pinning mechanisms in these conductors. Such an extended study is possible with the strain device that we introduce here, which allows us to measure J_c as a function of axial compressive and tensile strain, magnetic field and magnetic field angle at various temperatures.

2. Experiment

2.1. Sample preparation

YBCO coated conductors were purchased from SuperPower Inc. and consisted of ceramic buffer layers deposited on a 50 μm thick Hastelloy C-276 substrate. During fabrication, grain alignment was introduced into the MgO buffer layer with ion-beam-assisted deposition (IBAD). A 1.0 μm thick $Y_{0.9}Sm_{0.1}Ba_2Cu_3O_{7-\delta}$ layer was deposited on top of the buffer layers by metal-organic chemical-vapor deposition (MOCVD) [25, 26]. The Sm-doping in the YBCO layer enables the growth of high-density $(Y, Sm)_2O_3$ nanoprecipitate pinning centers that enhance flux pinning at 76 K [23, 24]. A silver cap layer, 2–3 μm thick, was deposited on top of the YBCO layer for electrical stability. The coated conductors were slit from a 12 mm wide tape to their final width of 4 mm. They were surround-plated with 20 μm of copper for electrical and thermal stability. The critical current density was about 3.2 MA cm^{-2} at 76 K and self-field.

2.2. In-field strain system

The in-field strain system consisted of a 98 wt%Cu–2 wt%Be bending spring that was about 10 cm in length and 1.3 cm in width (see figure 1), which is based on the principle that was first developed at the University of Twente in the Netherlands [27]. A 5 mm wide bridge was patterned in the spring, on top of which the YBCO coated conductor was soldered. The sample was strained within the elastic limits of the bending spring by moving the legs of the spring together (tensile strain), or apart (compressive strain) (see figure 2). The displacement of the legs was applied by a stepper motor that rotated a double-threaded stainless steel rod that was screwed in two threaded bushings connected to both legs. The rod consisted of a section of right-handed thread and a section of left-handed thread. The strain was measured with two strain gauges, one mounted on the bottom of the bending spring and one mounted on top of the sample. The strain profile through the cross section of the beam was determined with the two gauges. The strain in the YBCO layer was calculated with an uncertainty of 0.02% strain, using this strain profile and the position of the YBCO layer from the top surface (about 20 μm below the top strain gauge for the samples in this work). An example of the strain profile at the top surface of the spring that was calculated with a finite element analysis (FEA) program is presented in figure 2. The calculation shows that the strain at the surface of the spring was homogeneous over the length and width of the bridge. The strain will be fully transferred to the sample that was soldered on top of the spring, as long as the sample and solder thickness are small compared to the thickness of the beam, especially within the strain range below the strain at which the sample yields.

The bending spring and sample were located at the tip of a measurement probe, which was inserted in the center of an 8 T split-pair superconducting magnet. The magnetic field was oriented perpendicular to the spring and sample current, and the entire probe assembly was mounted on a rotating flange that was operated by a stepper motor. The magnetic field angle relative to the sample surface was changed by rotating the probe assembly in the magnet, while the magnetic field

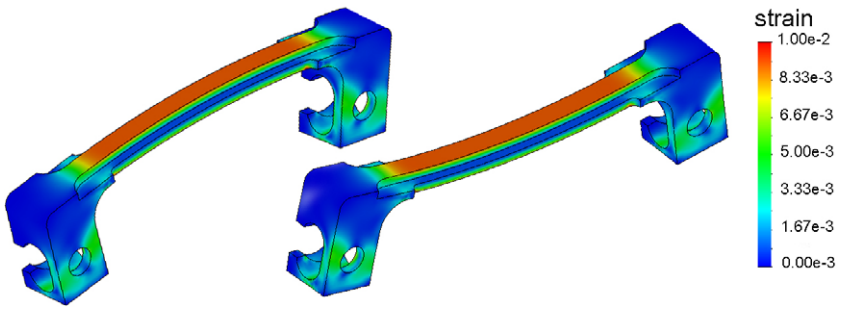

Figure 2. FEA-calculated strain profile of the bending spring for the two bending directions; +1% tensile strain (left) and −1% compressive strain (right). The analysis shows that the strain at the top surface of the beam where the sample is soldered is homogeneous over the length and width of the beam.

always remained perpendicular to the transport current in the sample. The stepper motor and flange were calibrated such that the angle between the field and the sample surface was always known. The magnitude and orientation of the magnetic field close to the center of the sample was also determined with two Hall sensors. The Hall sensors were mounted in the tip of the probe and were oriented 90° from each other, parallel and perpendicular to the sample surface. The magnetic field angle was determined within 1° uncertainty.

The probe was placed in a reentrant dewar with a narrow tail that separated the liquid helium bath of the superconducting magnet from the liquid nitrogen bath of the sample. The temperature of the nitrogen bath slowly decreased over time from its boiling point to about 73 K, even though the insert dewar was vacuum insulated from the helium bath. The sub-cooling of the nitrogen bath enabled a precise temperature control of the sample with a polyamide-encapsulated foil heater, even as the pressure of the bath changed with the height of the nitrogen column. The sample temperature was measured with a Cernox sensor attached to the bending spring. The temperature control was provided by the operating software that was developed specifically for this experiment. The sample temperature was kept at 75.90 ± 0.02 K when current was applied to the sample. Ohmic heating at the solder connections between superconducting current leads and sample raised the sample temperature by no more than 0.05 K at sample currents as high as 200 A.

The top part of the current leads to the sample were vapor-cooled with a current rating of 1000 A. Each vapor-cooled lead was connected to a superconducting current lead that consisted of a 25 mm wide by 1.6 mm thick copper bar on top of which six YBCO coated conductors were soldered. A connection from the fixed superconducting leads to the sample was made with flexible stacks of three YBCO coated conductors per lead. Both lead stacks were insulated and sandwiched together with thin fiberglass strips to provide support against the Lorenz force that occurs during measurements.

The measurement control and data acquisition were fully automated such that large data matrices could be taken in a relatively short period. The software controlled the stepper motors to achieve varying strain and magnetic field angle, as well as magnetic field and sample current. The critical current (I_c) of the sample was determined with a four-probe measurement with an uncertainty of 0.5% at an electric field criterion of 1 μV cm^{-1} by increasing the current stepwise through the superconducting transition. Typical data matrices included the measurement of critical current as a function of field angle at constant strain and magnetic field, the measurement of I_c as a function of strain at constant magnetic field and field angle, and the measurement of I_c as a function of magnetic field at constant strain and field angle.

3. Results

3.1. J_c as a function of magnetic field angle

To prevent damage to the conductor, we investigated the effect of strain on J_c, in the presence of a magnetic field, only for strains below the irreversible strain limit of about 0.7%.

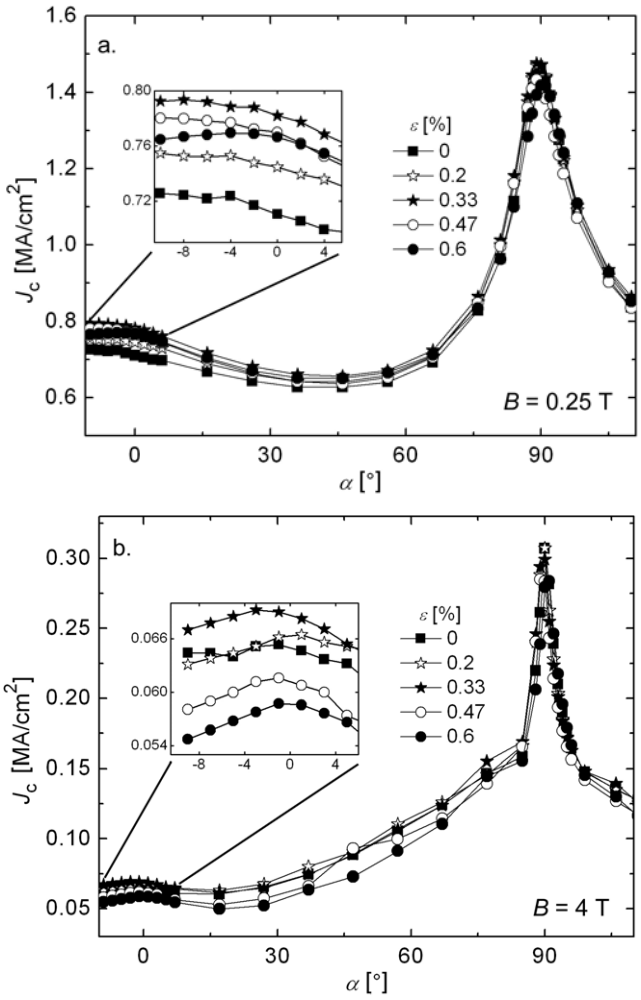

Figure 3. Angular dependence of J_c at 75.9 K and various levels of strain with an applied field of (a) 0.25 T and (b) 4 T. The part of the graph where magnetic field is applied parallel to the *c*-axis is enlarged in both figures.

The angular dependence of J_c at 75.9 K and a relatively low magnetic field of 0.25 T for five different strains is presented in figure 3(a). The angle at which the critical current density shows a large peak due to the high level of intrinsic flux pinning between the *ab*-planes of the YBCO is defined as 90°. The peak in J_c that is due to correlated defects when the field is applied parallel to the *c*-axis is expected to be at 0°. Both peaks are not always separated by 90° because the (Y, Sm)$_2$O$_3$ precipitate planes present in these conductors contribute to the pinning along the *ab*-planes. The (Y, Sm)$_2$O$_3$ precipitate planes are oriented at a 5° angle to the *ab*-planes [24] and shift the *ab*-peak away from 90° at low fields. The two peaks in the angular dependence of J_c are separated by roughly 90° when the magnetic field is increased to 4 T (see figure 3(b)), which shows that, at this field, the pinning between the *ab*-planes dominates over that at the (Y, Sm)$_2$O$_3$ precipitate planes.

The critical current density increases with tensile strain when a magnetic field of 0.25 T is applied along the *c*-axis of the conductor and reaches a maximum at about 0.4% strain (see inset of figure 3(a)). The increase in J_c with strain when the field is parallel to the *c*-axis is much smaller when the magnetic

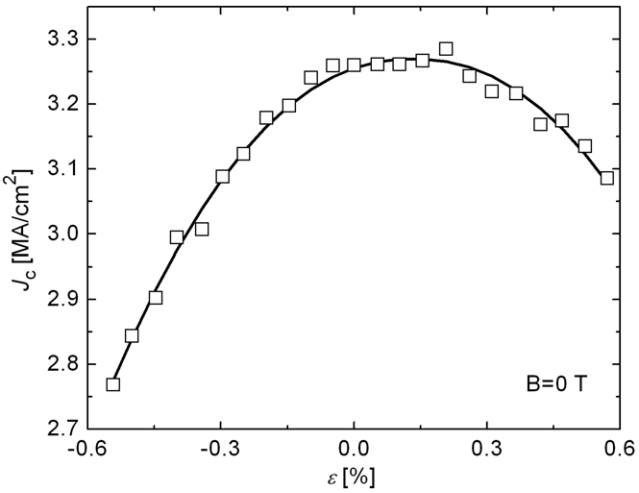

Figure 4. Strain dependence of J_c at 75.9 K in self-field within the strain range at which J_c changes reversibly. The solid line is a fit to the data according to equation (1).

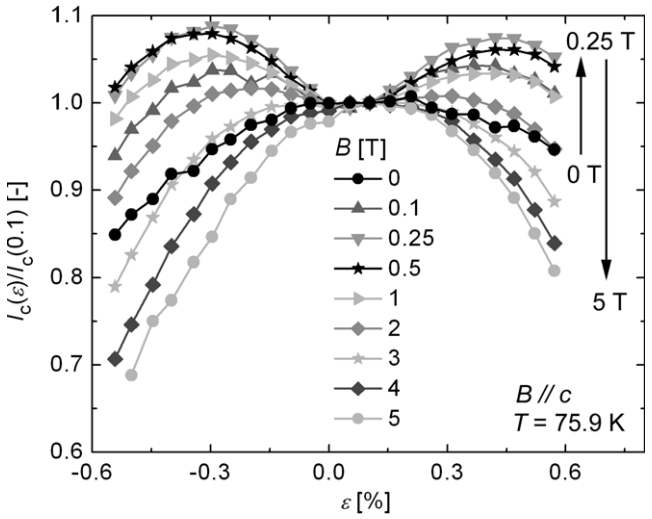

Figure 5. Critical current density at 75.9 K, normalized to its value at 0.1% strain, as a function of strain at various magnetic fields parallel to the c-axis.

field is raised above about 3 T (see inset of figure 3(b)). No significant increase in J_c with strain occurs when the magnetic field is applied parallel to the ab-planes; instead J_c decreases with strain for all magnetic fields.

3.2. J_c as a function of axial strain

The critical current density as a function of axial strain between about −0.55% compression and 0.55% tension in self-field is presented in figure 4. The change in J_c is fully reversible within this strain range: J_c fully recovers when the strain is removed (not shown). The strain dependence of J_c is described by the following power-law fitting function [12]:

$$J_c(B, \varepsilon) = J_c(B, 0)(1 - a(B)|\varepsilon - \varepsilon_m(B)|^{2.2\pm0.02}). \quad (1)$$

Parameter $a(B)$ represents the strain sensitivity of J_c, while $\varepsilon_m(B)$ represents the location of the peak in J_c that is related to the initial strain state of the YBCO layer [12, 28–30]. In this case, the peak occurs at about 0.13% tension, which would indicate that the YBCO layer is under −0.13% compressive strain after cool-down, due to differential thermal contraction.

A detailed study of the effect of magnetic field on the strain dependence of J_c was performed in the cases where the magnetic field is applied parallel to the c-axis and parallel to the ab-planes of the conductor. Both peaks in J_c occur at these field orientations for fields above about 3 T, where pinning in the ab-planes dominates over that in the $(Y, Sm)_2O_3$ precipitate planes. The magnetic field angle was kept constant in both cases, while the strain dependence of J_c was measured at different magnetic fields. The strain dependence of the normalized J_c over a strain range from −0.55% to 0.55% is shown in figure 5 for various magnetic fields applied parallel to the c-axis of the YBCO, and in figure 6 for fields applied parallel to the ab-planes. In both cases, the critical current density is normalized to its value at 0.1% strain, which is close to the strain at which J_c is maximal in the absence of an external field (see figure 4).

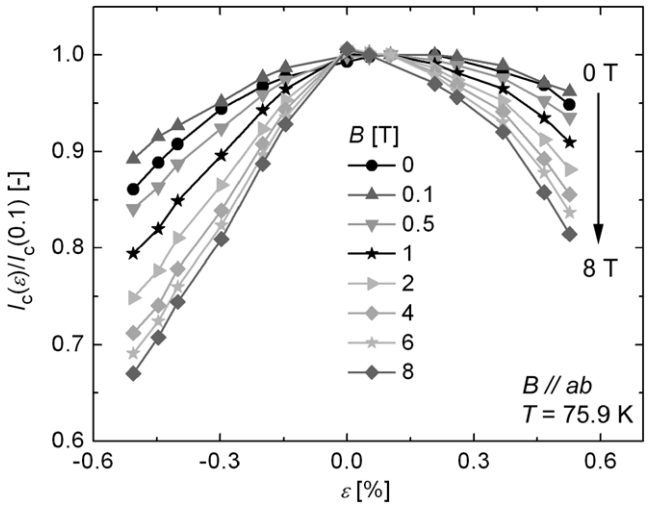

Figure 6. Critical current density at 75.9 K, normalized to its value at 0.1% strain, as a function of strain at various magnetic fields applied parallel to the ab-planes.

The critical current density versus strain shows two maxima when the magnetic field is applied parallel to the c-axis of the YBCO layer at low magnetic fields (see figure 5). Both maxima are located at strains of about −0.35% and about 0.45%, which is almost symmetric around the strain at which J_c is normalized ($\varepsilon = 0.1\%$). The relative magnitude of J_c at both peaks increases with magnetic field and reaches a maximum at about 0.25 T. The relative magnitude of the peaks decreases with magnetic field above 0.25 T, and both peaks disappear at an applied field of about 3 T. At 5 T, J_c decreases by about 30% when −0.5% compression is applied, while the reduction in J_c in self-field is only about 13% at that strain.

In the case where the field is applied parallel to the ab-planes of the YBCO, there is no increase in J_c with strain (see figure 6). The rate at which J_c decreases reversibly with both compressive as well as tensile strain increases with magnetic

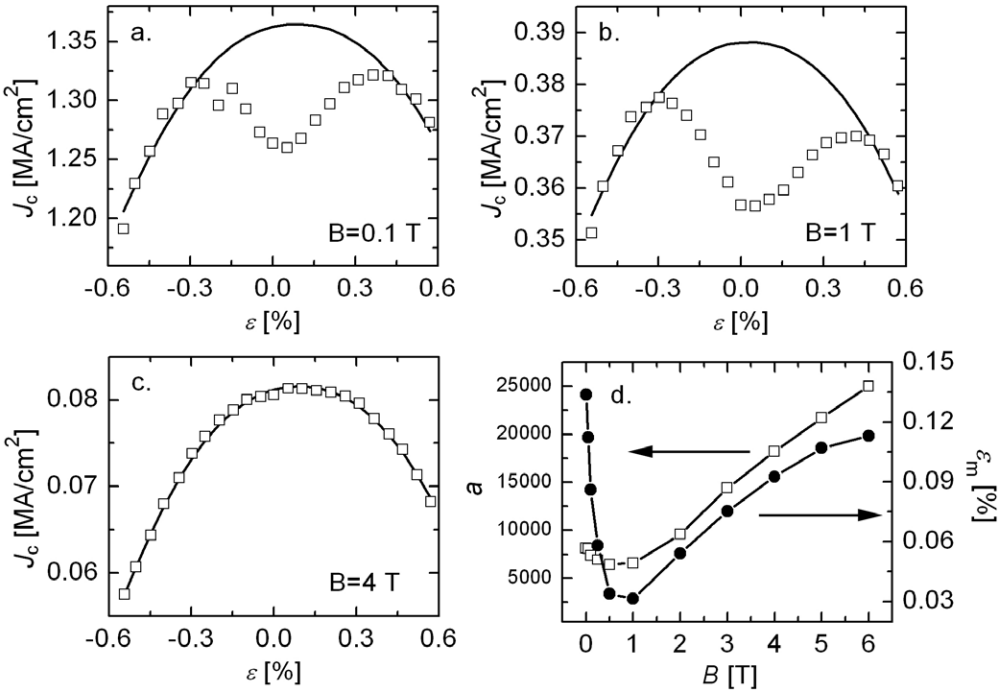

Figure 7. Critical current density at 75.9 K as a function of strain at magnetic fields applied parallel to the c-axis; (a) 0.1 T, (b) 1 T and (c) 4 T. The solid lines are a fit to the data according to equation (1). (d) Magnetic field dependence of the strain sensitivity parameter a, and the strain at which the peak in J_c occurs (ε_m) that is obtained from the fit of equation (1).

field. J_c decreases by more than 30% at -0.5% compression and for 8 T applied parallel to the ab-planes, compared to only 13% in self-field.

The effect of magnetic field on the intrinsic strain effect of J_c is studied in more detail by use of equation (1). The change in strain sensitivity a, and the strain at which J_c is maximal (ε_m) with magnetic field is obtained from this fitting function. The strain dependence of J_c for selected magnetic fields applied parallel to the c-axis of the YBCO is shown in figure 7, along with a fit to the data, according to equation (1). At applied fields of 0.1 T (figure 7(a)) and 1 T (figure 7(b)), a deviation from the fit within the strain range of about -0.4% compression to about 0.4% tension occurs, while equation (1) describes the data very well outside this strain range. The data points between -0.4% and 0.4% strain are not included in the fit at low magnetic fields. The deviation suggests that, at low magnetic fields parallel to the c-axis of the YBCO, J_c is suppressed within a strain range of about -0.4% to about 0.4%. This suppression does not occur at magnetic fields above 3 T, which becomes clear from figure 7(c), where the strain dependence of J_c at 4 T is fitted with equation (1) over the entire strain range.

The suggestion that J_c at low field and strain is suppressed is supported by the magnetic field dependence of the fitting parameters of equation (1) presented in figure 7(d). Parameters $a(B)$ and $\varepsilon_m(B)$ decrease with field below 1 T when the field is applied parallel to the c-axis, indicating a decrease in strain sensitivity, while both parameters increase with field for fields above 1 T, indicating an increase in strain sensitivity. The strain sensitivity parameter $a(B)$ decreases from about 8050 at self-field to about 6430 at 0.5 T and increases to over 25 000 at 6 T. The strain sensitivity of J_c increases by a factor of more than 3 at 6 T, compared to self-field.

Surprisingly, the strain (ε_m) at which the peak in J_c occurs is field dependent as well. It decreases from about 0.13% at self-field to about 0.03% at 1 T and then increases to about 0.11% at 6 T. This observation is made possible only by measuring J_c under compressive as well as tensile strain. As mentioned earlier, ε_m is thought to be related to the initial strain state of the YBCO and therefore is expected to be field independent. A change in ε_m with magnetic field has been reported previously [16], although the value of ε_m at low field was defined as the location of the peak in J_c under tension. The two maxima in J_c at low magnetic field were not observed, since the experiment was limited to tensile strain only. Still, the conclusion of [16] holds, namely that the location of the peak in the strain dependence of J_c is field dependent and thus not fully determined by the initial strain state of the YBCO layer.

The strain dependence of J_c at different magnetic fields applied parallel to the ab-planes is fitted with equation (1) in figures 8(a)–(c). A double peak in J_c with strain is absent, and equation (1) describes the data well over the entire strain range. The strain sensitivity of J_c, expressed by parameter a in equation (1), increases from about 6700 at 0.1 T to about 21 900 at 8 T (see figure 8(d)). The strain at which the peak in J_c occurs (ε_m in equation (1)) decreases almost linearly with magnetic field, from about 0.13% at self-field to about 0.10% at 8 T.

4. Discussion

A deeper understanding of the in-field strain effect is obtained when the effect is measured over an extended strain range that

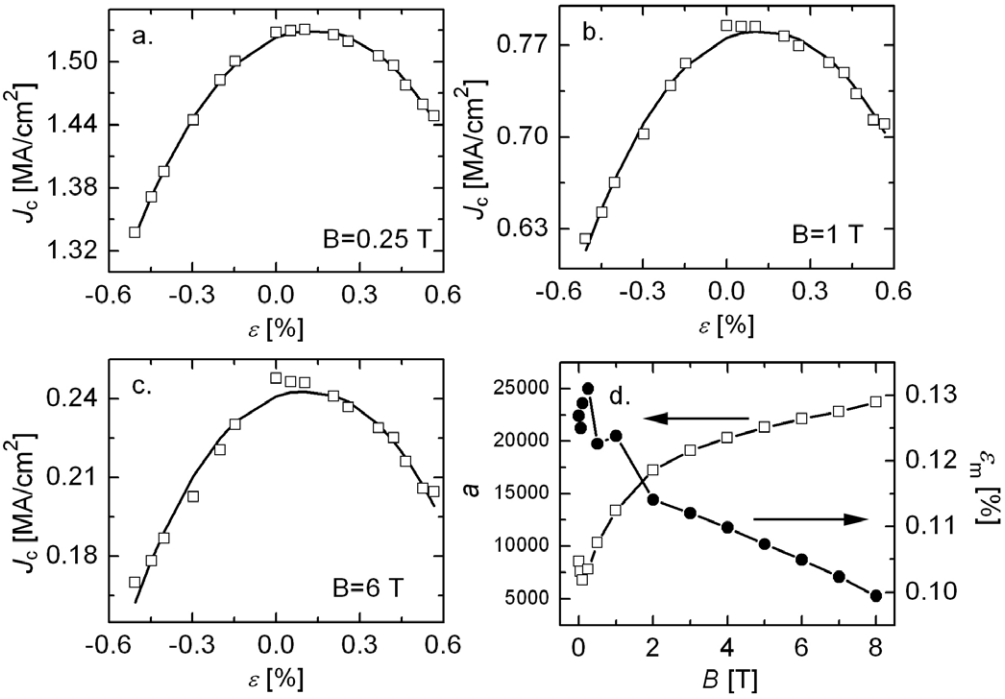

Figure 8. Critical current density at 75.9 K as a function of strain at magnetic fields parallel to the *ab*-planes; (a) 0.25 T, (b) 1 T and (c) 6 T. The solid lines are a fit to the data according to equation (1). (d) Magnetic field dependence of the strain sensitivity parameter a, and the strain at which the peak in J_c occurs (ε_m).

includes both compressive and tensile strain. For instance, the increase in J_c with strain as reported in [13, 14] is a direct consequence of the normalization of their J_c versus strain data at zero strain. The maximum in J_c with strain in self-field for copper laminated conductors that were measured in these studies occurs at about 0.1% tensile strain, which becomes clear only when the strain dependence of J_c is measured under compressive strain as well [12]. The change in height and location of the peak in J_c with strain and increasing magnetic field, as reported in [13, 14], is caused by the field dependence of $\varepsilon_m(B)$, which becomes clear only when J_c is measured under compressive strain as well. This shift in ε_m with field can be as large as 0.2% between self-field and 8 T in YBCO coated conductors that are produced with metal-organic deposition [31], compared to only about 0.03% in the YBCO coated conductors of this study that are produced with MOCVD.

Whether a change in critical temperature (T_c), and upper critical field (H_{c2}) with strain cause the intrinsic strain effect of J_c and its dependence on magnetic field remains unknown. The results of the current study show the importance of the strain characterization of J_c under compressive as well as tensile strain. Also, the ability to vary the magnetic field angle is important, since it is now clear that different pinning mechanisms in YBCO coated conductors are affected differently by strain. The cross-over in magnetic field dependence of parameters $a(B)$ and $\varepsilon_m(B)$ at about 0.5–1 T for fields parallel to the c-axis suggests the involvement of two different strain dependent pinning mechanisms. These mechanisms could be the pinning of Abrikosov–Josephson vortices at grain boundaries that dominates the field dependence of J_c at low magnetic field, and pinning of Abrikosov-vortices within the grains that dominates at high field [32]. YBCO coated conductors are complex granular systems, and a deeper understanding of the effect of strain on the different pinning mechanisms in YBCO can be obtained only when well-defined structures such as YBCO thin films on single- and bi-crystalline substrates are studied [28].

5. Conclusions

A new device has been constructed that allows the study of the intrinsic strain effect on the critical current density of YBCO coated conductors in the presence of a magnetic field. The effect of axial compressive and tensile strain on the various pinning mechanisms that form the complex pinning landscape of these conductors can be studied by varying the angle at which the magnetic field is applied. Initial results show that the reversible reduction in critical current density with strain is enhanced by the presence of a magnetic field for all field angles. The critical current density is reduced by about 30% at −0.5% strain when a magnetic field of 5 T is applied parallel to the c-axis of the conductor, or at 8 T when the field is applied within the *ab*-planes, compared to a reduction of only 13% in self-field. This reduction may have significant implications for applications where the conductor experiences large axial stresses in the presence of a magnetic field.

Differences in strain dependence of the critical current density when the magnetic field is parallel to the c-axis, compared to when it is parallel to the *ab*-planes show that the various pinning mechanisms in YBCO coated conductors are affected differently by strain. A double maximum in critical current density with strain occurs at low magnetic

fields parallel to the *c*-axis of the conductor, which indicates a suppression in critical current density at low strains. This behavior likely originates from the strain dependence of grain boundary flux pinning, and is not observed when the magnetic field is applied parallel to the *ab*-planes of the YBCO. The strain at which the critical current density is maximal shifts with magnetic field, and depends on the angle at which the magnetic field is applied. This indicates that the location of the peak in J_c with strain is not entirely determined by the initial strain state of the YBCO layer.

Acknowledgments

This work was supported in part by the US Department of Energy, Office of Electricity Delivery and Energy Reliability. Certain commercial materials are referred to in this paper to foster understanding. Such identification implies neither recommendation or endorsement by NIST, nor that the materials identified are necessarily the best available for the purpose.

References

[1] Selvamanickam V *et al* 2008 *Physica* C **468** 1504–9
[2] Malozemoff A P *et al* 2008 *Supercond. Sci. Technol.* **21** 034005
[3] van der Laan D C, van Eck H J N, ten Haken B, ten Kate H H J and Schwartz J 2003 *IEEE Trans. Appl. Supercond.* **13** 3534–9
[4] Sugano M, Osamura K, Prusseit W, Semerad R, Itoh K and Kiyoshi T 2005 *IEEE Trans. Appl. Supercond.* **15** 3581–5
[5] Sugano M, Osamura K, Prusseit W, Semerad R, Itoh K and Kiyoshi T 2005 *Supercond. Sci. Technol.* **18** S344–50
[6] Sugano M, Machiya S, Osamura K, Adachi H, Sato M, Semerad R and Prusseit W 2009 *Supercond. Sci. Technol.* **22** 015002
[7] van der Laan D C 2009 *Supercond. Sci. Technol.* **22** 065013
[8] van der Laan D C, Ekin J W, Clickner C C and Stauffer T C 2007 *Supercond. Sci. Technol.* **20** 765–70
[9] van der Laan D C and Ekin J W 2008 *Supercond. Sci. Technol.* **21** 115002
[10] Garcia-Moreno F, Usoskin A, Freyhardt H C, Wiesmann J, Dzick J, Heinemann K and Hoffmann J 1997 *Inst. Phys. Conf. Ser.* **158** 1093–6
[11] Cheggour N, Ekin J W, Clickner C C, Verebelyi D T, Thieme C L H, Feenstra R and Goyal A 2003 *Appl. Phys. Lett.* **83** 4223–5
[12] van der Laan D C and Ekin J W 2007 *Appl. Phys. Lett.* **90** 052506
[13] Cheggour N, Ekin J W and Thieme C L H 2005 *IEEE Trans. Appl. Supercond.* **15** 3577–80
[14] Cheggour N, Ekin J W, Thieme C L H, Xie Y-Y, Selvamanickham V and Feenstra R 2005 *Supercond. Sci. Technol.* **18** S319–24
[15] Uglietti D, Seeber B, Abacherli V, Carter W L and Flukiger R 2006 *Supercond. Sci. Technol.* **19** 869–72
[16] Sugano M, Nakamura T, Manabe T, Shikimachi K, Hirano N and Nagaya S 2008 *Supercond. Sci. Technol.* **21** 115019
[17] Civale L *et al* 2004 *Physica* C **412** 976–82
[18] Civale L *et al* 2004 *Appl. Phys. Lett.* **84** 2121–3
[19] Civale L *et al* 2005 *IEEE Trans. Appl. Supercond.* **15** 2808–11
[20] Song X *et al* 2006 *Appl. Phys. Lett.* **88** 212508
[21] Gutierrez J, Puig T and Obradors X 2007 *Appl. Phys. Lett.* **90** 162514
[22] Gutierrez J *et al* 2007 *Nat. Mater.* **6** 367–73
[23] Chen Z *et al* 2007 *Supercond. Sci. Technol.* **20** S205–10
[24] Chen Z, Kametani F, Chen Y, Xie Y, Selvamanickam V and Larbalestier D C 2009 *Supercond. Sci. Technol.* **22** 055013
[25] Selvamanickam V 2001 *IEEE Trans. Appl. Supercond.* **11** 3379–82
[26] Selvamanickam V, Xie Y, Reeves J and Chen Y 2004 *MRS Bull.* **29** 579–82
[27] ten Haken B, Godeke A and ten Kate H H J 1997 *J. Appl. Phys.* **85** 3247
[28] van der Laan D C, Haugan T J and Barnes P N 2009 *Phys. Rev. Lett.* **103** 027005
[29] Osamura K, Sugano M, Machiya S, Adachi H, Ochiai S and Sato M 2009 *Supercond. Sci. Technol.* **22** 065001
[30] van der Laan D C, Haugan T J, Barnes P N, Abraimov D, Kametani F, Larbalestier D C and Rupich M W 2010 *Supercond. Sci. Technol.* **23** 014004
[31] van der Laan D C, Douglas J F, Clickner C C, Stauffer T C, Goodrich L F and van Eck H J N 2010 Origin of the reversible strain effect on critical current density and flux pinning in $Bi_2Sr_2Ca_2Cu_3O_x$ tapes *Phys. Rev. Lett.* submitted
[32] Gurevich A and Cooley L D 1994 *Phys. Rev.* B **50** 13563–76